

Jennifer Rico Varela

**"Optimizing Oxygen Concentrations In Situ: Enzymatic
Oxidation Reaction in Continuous Microreactors"**

MARSHALL PLAN
SCHOLARSHIP PAPER

Supervisors:

Univ.-Prof.Dipl.-Ing.Dr.techn.Bernd Nidetzky

and

Dr. Juan Manuel Bolivar

Institute of Biotechnology and Biochemical Engineering,
Graz University of Technology



Graz, November 2013

©Copyright by Jennifer Rico Varela

Content Page

1. Abstract	3-4
2. Introduction	5-7
3. Methods and Materials	8-17
3.1 Materials	8-11
- <i>Dyes and Nanoparticles</i>	8
- <i>Enzymes and Hydrogen Peroxide Preparation</i>	8-10
- <i>Microreactor Assembly</i>	10-11
3.2 Methods	11-17
- <i>Nanoparticles Preparation</i>	11
- <i>Nanoparticles Characterization</i>	11-12
- <i>Continuous Microreactor Set Up</i>	13
- <i>Continuous Oxidation of Glucose Inside the Microreactor</i>	13-14
- <i>Real Time Lifetime Imaging</i>	15-16
- <i>Modeling and simulation of continuous microreactor</i>	16-17
4. Results and Discusssion	18-26
- <i>Characterization of Size of Nanoparticles</i>	18
- <i>Characterization of Nanoparticles</i>	18-19
- <i>Modeling Results</i>	19-20
- <i>Analysis of Glucose Conversion with and without particles</i>	21-23
- <i>Analysis Real Time Lifetime Imaging</i>	23-26
5. Conclusions and Outlook	27-28
6. Acknowledgements	29
7. References	30-31

1. Abstract

The control of a suitable local oxygen concentration is essential to meet different biotechnological requirements. Enzyme-catalyzed oxidations are usually highly limited by very low local oxygen concentrations and an efficient system of oxygen delivery to the heterogeneous catalyst is critical. The use of continuous microreactors is a promising, powerful, engineering strategy since reaction intensification in heterogeneous biotransformations may be achieved at the microscale. One smart strategy for in situ oxygen supply is the integration of a complementary biochemical reaction as hydrogen peroxide decomposition catalyzed by catalase. The study of optimal combination of glucose oxidase, catalase, hydrogen peroxide (H_2O_2) concentrations and operation variables (flow) drove to an optimal operation window with a controlled defined oxygen concentration in the microreactor. The microreactor was integrated with an advanced luminescence technique for oxygen imaging. Nanosensor particles (containing luminescence oxygen sensitive indicators) were used in flow and the system interfaced with in situ lifetime microscopy. Nanoparticles containing Iridium Coumarin or $Ir(Cn)_2(acac)$ were found to be more suitable for lifetime imaging than Platinum Porphyrin or PtTFPP (1%) since these require more optimization for the desired measurements. The reactions were performed with in situ oxygen resolution and followed by glucose conversion under steady state conditions. These first studies lead to the determination of conditions where the microreactor is with oxygen concentration depleted (inefficient glucose conversion) and conditions where the system is saturated with oxygen (highly efficient glucose conversion). These preliminary results suggest that H_2O_2 concentration and catalase activity are critical parameters to enhance glucose conversion. The use of equivalent activities of glucose oxidase and catalase (20 units/mL) lead to the control of reaction by H_2O_2 concentration. Thus, glucose conversion under particles absence

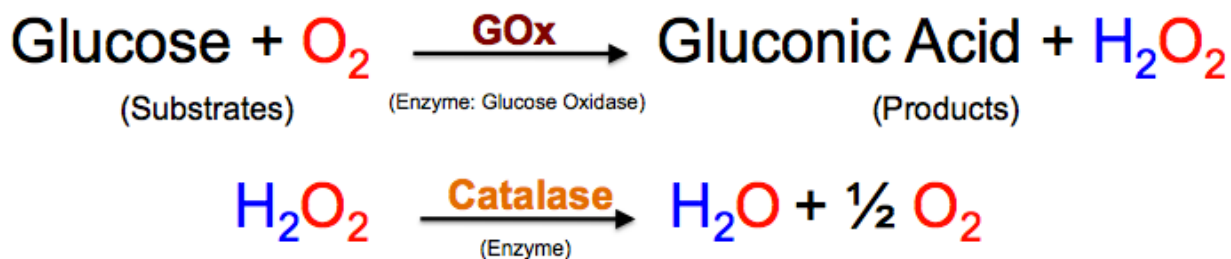
matched predicted conversion as opposed to conversion under particles presence. In addition, oxygen generation in situ was achieved successfully but since glucose conversion was affected by particles, thus oxygen conversion was highly affected under high concentrations of hydrogen peroxide.

2. Introduction

Molecular oxygen is an important parameter in many biological and biotechnology applications. In the case of biological systems, oxygen presence is very important for cell behavior and functioning. For instance, it is required for many biological processes such as respiration, aerobic metabolism, and activation of enzymes to bring homeostasis to the body [1-4]. In biotechnology, molecular oxygen plays an important role for aerobic applications such as evolving bioreactors which are indispensable for oxygen transfer, for instance, among microorganism [5]. Enzymes are a type of catalyst, useful in the production of substance in an environmentally friendly way. They also have high potential for analytical applications. However, not all enzymatic processes have been commercialized due to stability problems of the enzymes, cost, and efficiency of the reactions[6]. Thus, there have been demands for innovation in biotechnology, and biochemical engineering, particularly for enzymatic reactions, and continuous microreactors. For instance, molecular oxygen is the co-substrate of enzyme-catalyzed oxidations. Oxidations are usually highly limited by very low local oxygen concentrations under different catalyst and reactor configuration [7] and an efficient system of oxygen delivery to the catalyst is critical [7, 8].

Microfluidic devices had led the next technology of the mid-20th century with promising advantages in a diverse field of research, including biotechnology [9, 10]. These devices allow controllable volumes, and are low-priced and easy to integrate with other components (e.g. valves, pumps, nanoparticles, etc) [9, 11]. Measurements within microfluidic devices or continuous microreactors have the potential to be reproducible and controllable for repeatability, and long-term experiments. These characteristics allow for a suitable control of oxygen levels on-chip. In order to control oxygen concentrations locally in continuous microreactors, one

interesting strategy proposed in this study is the oxidation of glucose through glucose oxidase (GOx) lead to hydrogen peroxide. Then, this toxic by-product (in the case of cell respiration) would be removed by catalase to produce one-half molecule of oxygen as shown by the equation below. With this simple strategy, it is intended to generate oxygen in situ without saturating the microenvironment. Thus, the strategy for continuous in situ oxygen supply consists of the integration a complementary reaction between hydrogen peroxide decomposed by catalase. Without this feeding strategy, a trustable glucose conversion would not be possible (higher glucose conversion). In addition, this feeding strategy would be driven primarily for the proper balance between the enzymatic activities of GOx and catalase along with different concentrations of hydrogen peroxide. In other words, determining the proper amounts of glucose, GOX, catalase and hydrogen peroxide help to enhance a system with controllable amounts of oxygen



To determine oxygen concentrations in situ, selecting the method of quantification plays an important role. Oxygen measurements have been established before, through optical techniques such as ratiometric and lifetime imaging [12, 13]. In both cases, the use of optical oxygen-sensing particles is crucial to image oxygen tension over a certain area of interest. The ratiometric approach applies the principle of light harvesting by utilizing the red and green channel of a color camera [9]. The lifetime approach measures the average time nanoparticles spend in the excited state after being excited with an LED at specific thresholds and times before

returning to their ground state. For this work, lifetime imaging was selected over ratiometric imaging since this approach was not tested before for oxygen detection using enzymatic reactions and nanoparticles in flow as sensors.

For this work, two different nanoparticles were experimentally tested (Iridium coumarin and platinum porphyrin) to determine the more luminescent particles that can reduce signal to noise ratio during data analysis. In this work, Ir(Cs)₂acac nanoparticles were reported to be the optimal oxygen nanosensor to measure oxygen concentrations in situ in a continuous microreactor based on their size, characterization, and outcomes during optical measurements as compared to platinum porphyrin. These particles have been previously tested, and were found to have higher quantum yield and efficient visible absorption [14].

3. Materials and methods

3.1. Materials:

Dyes and Nanoparticles: For this work, two oxygen-sensitive luminescent dyes were used and synthesized at the Institute of Analytical Chemistry and Food Chemistry – TU Graz, as previously described by Borisov et al. (2007). These dyes are: Iridium(III)((Benzothiazol-2-yl)-7-(diethylamino)-coumarin))2(acetylacetonat) or most commonly known as Ir(Cs)2(acac) (see Figure 1(a)), and Platinum Porphyrin or Platinum(II)-5,10,15,20-tetrakis-(2,3,4,5,6-pentafluorophenyl)-porphyrin (also known as PtTFPP) (See structure in Figure 1(b)), [13, 14]. These dyes were used to stain nanosensor particles or luminescent poly(styrene-block-vinylpyrrolidone) nanobeads or PSPVP according to the literature procedure previously described by the same institute [15].

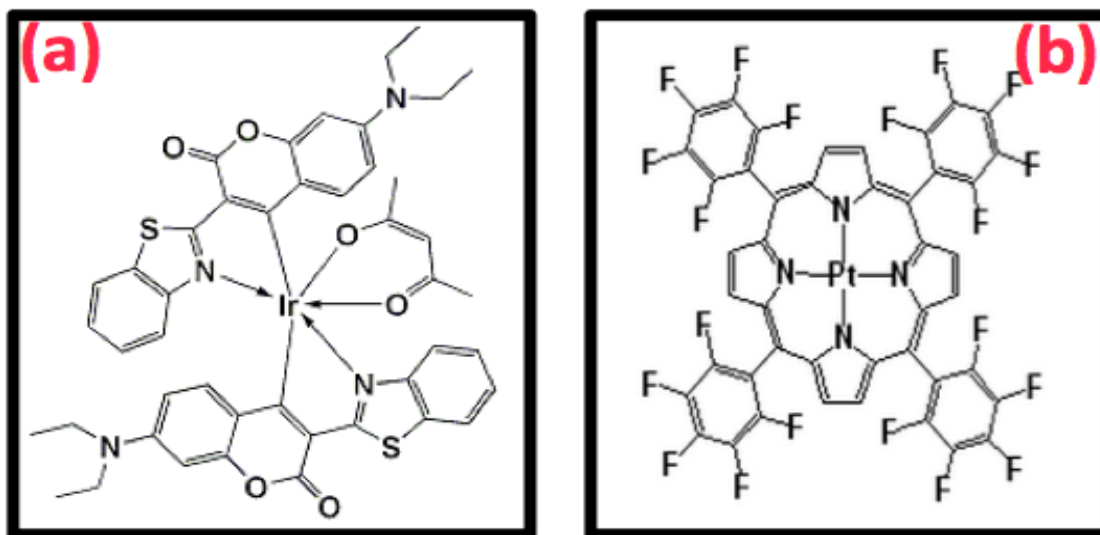


Figure 1. Chemical structure of (a) Ir(Cs)2(acac) and (b) PtTFPP.

Enzymes and Hydrogen Peroxide Preparation: Glucose oxidase (GOx) from *Aspergillus niger* (Sigma Aldrich, St. Louis, Missouri, Cat. No. G7141), and catalase from bovine liver (Sigma

Aldrich, St. Louis, Missouri, Cat. No. C9322-1G), were prepared to possess the same volumetric enzymatic activity throughout all measurements. At first, of 20 units/mL of each enzyme (GOx and catalase) were used when the flow rate was 1 μ L/min. Then, enzymes' activity was changed as a result of increasing the flow rate three times (activity used in both enzymes 60units/mL) to adjust low signal acquisition (more details on Real Time Lifetime Imaging section).

To determine the enzymatic activity of GOx over time, oxygen consumption rates were measured. In this case, oxygen bulk concentration was followed via a fiber-optic oxygen micro-optode (MICROX TX3, PreSens GmbH, Regensburg Germany)[16, 17]. This fiber-optic sensor was placed inside an open glass vial filled with 3.8mL of 50mM potassium phosphate (buffer solution) and 200 μ L of 2.5mM glucose at 30°C under continuous magnetic stirring (300rpm). After one minute of recording data with P500V520 Software, oxygen signal was stable and 20 μ L (1:5 dilution) of GOx were added to the vial. The last step consisted of determining the slope of the line after a series of calculations to determine the amount of enzyme (1 unit of GOx) required to produce 1 μ mol of hydrogen peroxide per minute.

To determine the enzymatic activity of catalase over time, a UV-spectrophotometer (Varian Inc., CARY 50 Bio, The Netherlands) was used to determine the amount of enzyme (1 unit of catalase) required to produce one molecule of water and $\frac{1}{2}$ molecule of molecular oxygen per minute. Using the Kinetics Software, absorbance vs wavelength were displayed after blanking one cuvette with 50mM buffer solution, and then adding 10 μ L (1:30 dilution) of catalase after one minute. The resulting slope, after a series of calculations, represents the activity of catalase.

Finally, D-(+)-glucose monohydrate (C. Roth, Karlsruhe, Germany, Cat. No. X997.3) had molar concentration of 200mM in all experiments. Another important reagent was 30% Hydrogen Peroxide (C. Roth, Karlsruhe, Germany, Cat. No. 9681.1); all these substances were prepared in 50mM buffer pH 7 solution.

Microreactor set-up: A powderblasted microreactor made of optically transparent glass that allowed for the visualization of the inner microchannels was used to carry out all optical measurements. These microchannels were rectangular and curved at the edges to facilitate the total length of 760mm. In addition, the microreactor had a cross sectional area of 150x150 μ m in both, channel width and depth, with a maximum volume capacity of 13 μ L (Micronit Microfluidics B.V., Enschede, The Netherlands, Cat. No. FC_R150.676.2). This microchip was composed of two inlet channels which converged together to form a central channel, and one outlet channel at the end of device as shown in Figure 2.

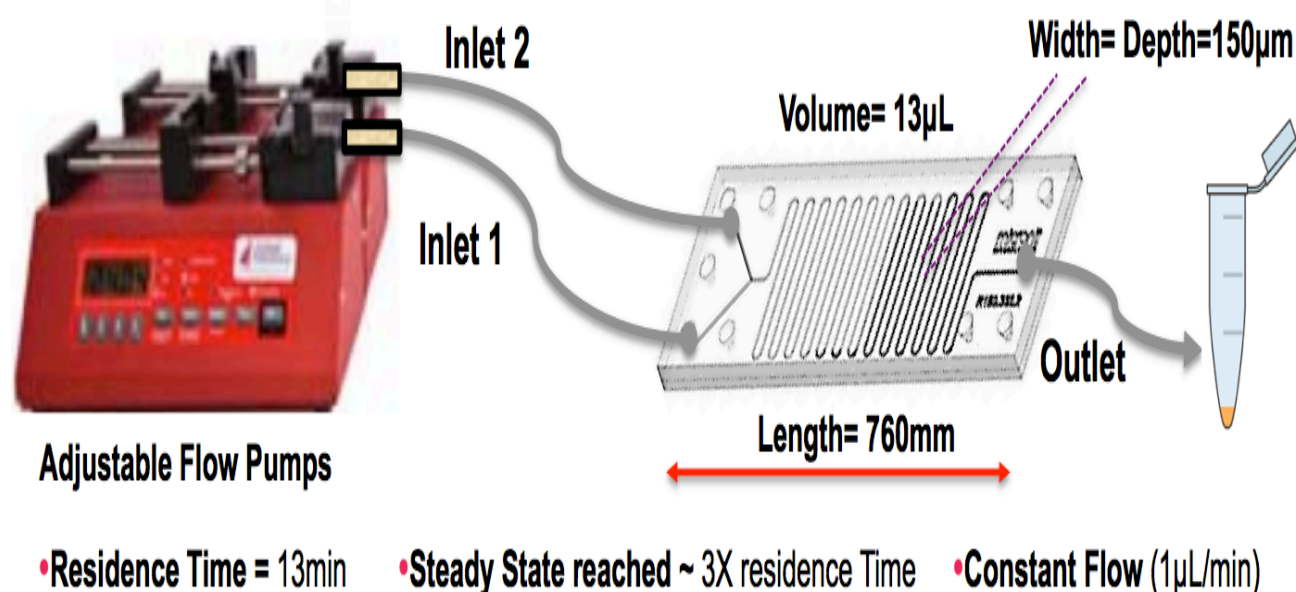


Figure 2. Illustration of the set up for the continuous flow microreactor (from Micronit Microfluidics). It is composed of two inlets and an outlet.

Likewise, it was composed of an outlet at the end of the device. Furthermore, a chip holder made of stainless steel was used to position the microchip inside as well as to prevent leakage at the inlets and outlets. The housing of device was connected with a Teflon tubing of 0.25mm in diameter; each tube was connected to the two inlets and the outlet individually (approximately 10cm in length each tube). The two tubes connected to the inlets were hooked up to two 2-mL syringes, and through two SP1000 programmable syringe pumps (Next Advance Inc., Averill Park, New York), the flow rate in each syringe was controlled ($3\mu\text{L}/\text{min}$) with a resident time of almost 4 minutes. The system was expected to reach steady state after 3 times the residence time.

3.2. Methods:

Nanoparticles Preparation: Two sets of nanoparticles (platinum porphyrin and iridium coumarin) were separately prepared using the same amount of PSPVP, water and tetrahydrofurane (THF). Thus, five hundred and twenty six milligrams of 38% emulsion in water of PSPVP were diluted with the mixture of 50mL of water and 30mL of THF. In the case of Platinum Porphyrin, 1.93mg of platinum-complex (1%) and 5.65mg of macrolex yellow (3%) were mixed with 20mL of THF. In the case of Iridium coumarin, 2.63mg of it was mixed with 20mL of THF. This solution was added drop-by-drop using a glass Pasteur pipette under magnetic stirring of the polymer. Finally, a rotary evaporator removed all THF (50°C ; 400mbars; 175rpm) and water (70°C ; 200mbars; 175rpm), and the final suspension was diluted with 50mM buffer solution up to 20mL overall volume.

Nanoparticles Characterization: oxygen lifetime imaging was completed using a Zeiss Axiovert 25 CFL (Zeiss, Gottingen, Germany) adopting a CCD-Camera (Sensimod FastShutter, PCO, Kehlheim, Germany) to determine lifetime imaging [13, 18, 19]. A blue LED was incorporated into the equipment previous described. This LED has a maximum emission at 450nm

wavelength, used to trigger excitation light for fluorescence lifetime imaging as described by Ungerböck, et al. (2012). Both particles calibration took part outside the microreactor by pumping gaseous air-nitrogen and oxygen through a gas mixer. Different concentrations of these gases were used: decreasing air-nitrogen while increasing oxygen concentrations [mL/min] over a period of 32 minutes per batch of particles. In other words, higher air-nitrogen concentrations (nearly zero oxygen concentrations) represent fully deoxygenated conditions while higher oxygen concentrations (nearly zero nitrogen concentrations) represented fully air-saturated conditions. Both particles, platinum porphyrin and iridium coumarin, were characterized to determine the optimal sensor to continue with optical measurements. For both cases, Stern-Volmer Plots Calibration for each nanoparticle against partial oxygen concentrations [hPa] were provided in Figure 4 (c) and (d).

On the other hand, Zetasizer Nano Series (Malvern Instruments Ltd., Worcestershire, United Kingdom) was used to characterize both particles size. In order to determine the size of particles, this instrument first measured the *Brownian Motion* (random movement of particles in liquid due to surrounding molecules) of particles in a sample (1:10 dilution in 50mM buffer solution) using dynamic light scattering (DLS). This DLS measures particles' size by illuminating them with a laser and analyzing the variation of the light scattering [20]. Small particles (move quickly) possess a typical hydrodynamic diameter of less than 100nm while large particles have a diameter range between 100-1000nm [20]. By using Zetasizer Nano Series instrument, the size of both particles' sizes were measured six times, and the hydrodynamic diameter of each nanoparticle was reported as the mean \pm standard deviation by employing the Polydispersity Index (PDI) parameter to be significant when this value is less and equal to 0.05.

Continuous Microreactor Set Up: two syringes were prepared as follow: (1) 200mM glucose, 60 units/mL of GOx, 60 units/mL of catalase, and nanoparticles; (2) zero or different concentrations of hydrogen peroxide (40, 80, and 200mM) along with nanoparticles. In each syringe, volume of nanoparticles was maintained the same along all experiments. Thus, the maximum volume in each syringe was 500 μ L, which was pumped at a rate of 3 μ L/min. After 15 minutes (steady state reached), continuous oxidation of glucose inside the microreactor with and without nanoparticles presence was measured as well as lifetime imaging. It is important to mention that each concentration of hydrogen peroxide loaded in the syringes corresponded to half the desired concentration at the end of the reaction (e.g. 40mM loaded in the syringe but 20mM at the outlet).

Continuous Oxidation of Glucose Inside the Microreactor: glucose conversion was measured under the presence and absence of nanoparticles. Under the absence of nanoparticles, the microreactor was set up as described in the above section (Continuous Microreactor set up) but instead of particles, buffer solution filled both syringes up to 500 μ L. After all mixing took place inside the reactor, an eppendorf tube placed at the outlet, collected 1mL sample solution. The reaction was stopped with 1M of hydrochloric acid as sample solution was collected. From this sample solution, only 10 μ L were dissolved in 500 μ L of Hexokinase Dipromed Glucose Kit (as previously described in [21]) and measured NADH absorbance at 340nm using UV Spectrophotometer. These results presented as glucose conversion [mM], were obtained by dividing absorbance values (1:20 dilution) by 0.12 [21], which corresponds to the molar coefficient extinction (provided in the product sheet of glucose kit). Each experimental condition went through the same process after measuring absorbance at 340nm.

When particles were present in both syringes at equal volumes, it was observed that glucose concentration determination was highly affected by nanoparticles. In order to overcome this issue, a new calibration curved was generated after the centrifugation of each sample solution at 16,100rpm and 4°C for 35 minutes. After sample centrifugation, absorbance of each experimental condition was reported as glucose conversion data. This calibration curved was obtained from 10 different glucose concentrations [mM] within the range of 5-100mM, which were dissolved in buffer solution. This method allowed to isolate Ir(Cs)2acac particles from the sample solution and thusu obtain a better estimation of glucose conversion. The new calibration curve was displayed as the Absorbance vs Glucose concentrations [mM] plot, where the slope for Ir(Cs)2acac was reported to be 0.96 as shown in Figure 3.

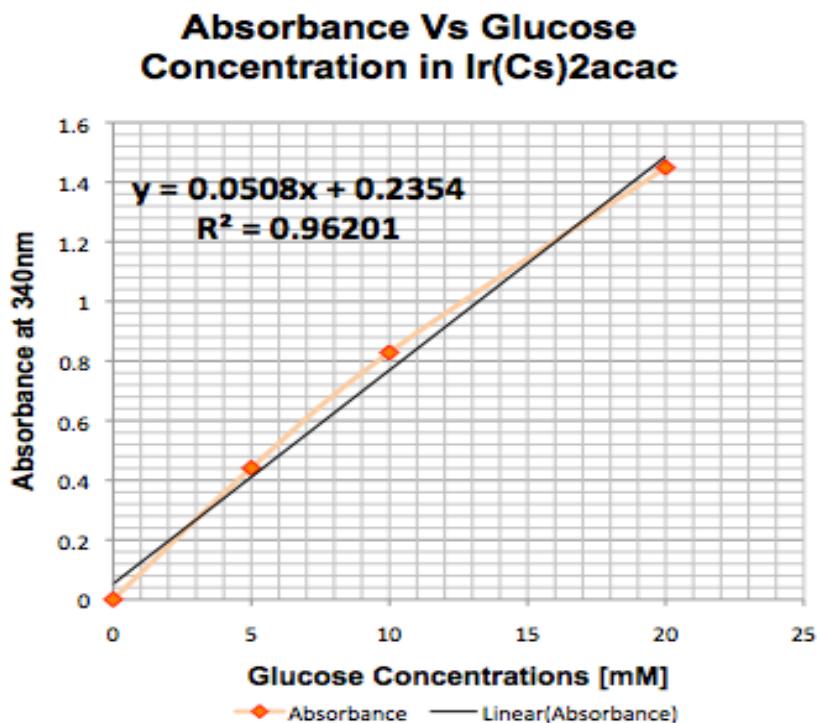


Figure 3. Calibration curve used for glucose conversion under particles presence.

Real Time Lifetime Imaging: an inverted microscope connected to a monochrome camera (as previously described [22]) was used to perform lifetime imaging measurements. In principle, Ir(Cs)₂acac nanoparticles were excited at 470nm wavelength emitted by a blue LED integrated into the filter cube of the microscope with an electronic shutter [12]. For measurements, the range of integration time was between 500-1000 milliseconds (higher exposure time for oxygenated cases). In addition, a “triggerbox” (assembled by Björn Grunwald, MPI Bremen, Germany) was the pulse generator for the LED and camera with an output current of 1.4 amperes and input voltage of 7 volts. This whole set up was connected to a computer where image processing and data acquisition was possible through Look@Molli v.1.83 software (Björn Grunwald, MPI Bremen, Germany). The following conditions used different exposure times but other important parameters were kept the same.

The oxygenated condition consisted of 200mM glucose and Ir(Cs)₂acac particles, only. In this case, an exposure time of 500 milliseconds was used. At first, the deoxygenated condition consisted of 200mM glucose and 20units/mL of GOx along with particles dissolved in buffer solution. The substrate (glucose) and GOx were loaded on different syringes. Due to low signal acquisition, it was proposed to increase the activity of GOx while the flow rate increased and the resident time decreased. Moreover, it was proposed to pre-mix glucose and GOx in the same syringe for future measurements as well as repeating the deoxygenated condition with 60units/mL of GOx with an exposure time of 500 milliseconds.

In situ conversions were obtained after collecting 30 images per position every minute. There were three positions selected for optical measurements: beginning, middle, and ending of device.

Each image taken contained 3 microchannels, and their lifetime values were processed with MatLab 7.7 (MathWorks, Natick, MA). The lifetime information was processed in the three regions of interest within the device (initial, middle, final position), so that oxygen measurements depend on this values (Table #2). The MatLab-scripts were adapted from the diploma thesis of Birgit Ungerböck (Graz University of Technology, 2012). In order to confirm lifetime values for the oxygenated and deoxygenated conditions, the values generated from the Stern-Vern Plots for Ir(Cs)₂acac against Partial Oxygen Concentrations [hPa] were used as a guide to monitor in situ measurements. After collecting lifetime values from MatLab, these were averaged per position, then normalized, and finally converted to oxygen concentrations in hepta-Pascal and umol/L. The control groups were the oxygenated and deoxygenated conditions in situ, which were used as a guide to measure 40mM, 80mM, and 200mM of hydrogen peroxide, independently (Table 2).

Modeling and Simulation of a Continuous Microreactor: The continuous microreactor was modeled as an ideal tubular continuous reactor (plug flow reactor) under steady state. Model was constructed to perform the simulation using Berkeley Madonna (f.Madonna version 9.0.110) including the glucose balance, oxygen balance and hydrogen peroxide balance. Code used was as follows:

```

d/dt (Oxygen) = - rgox*A/F + 0.5*rcat*A/F ; mM/cm ; O2 balance
d/dt (glucose) = -rgox*A/F ; mM/cm ; Glucose balance
d/dt (h2o2) = rgox*A/F -rcat*A/F ; mM/cm ;Hydrogen peroxide balance
RENAME Time=L ;cm ;Axial dispersion
rgox= Vmax*oxygen/oxygenzero*glucose/(KG+Glucose) ; mM/min,
Glucose oxidation kinetic
init oxygen= oxygenzero ; Inflow O2 concentration
init glucose= 100 ; Inflow glucose concentration
oxygenzero=0.25 ; mM, O2 solubility at 25 °C.
init h2o2= h2o2zero ; Inflow hydrogen peroxide concentration
kg=2 ; Saturation constant for glucose, mM

```


$A = 0.000225$;cm², Cross sectional are of channel
 $F = 0.001$; Flow, cm³/min
 $Total_L = 76$; Length of microreactor, cm
 $Total_volume = 0.013$;volume of microreactor, cm³
 $residence_time = total_volume/F$;Residence time, min
 $Vmax = 10$; Volumetric activity of Gox under substrate saturating conditions
 $rcat = vmaxcat * h2o2 / (kcat + h2o2)$; mM/min, hydrogen peroxide decomposition kinetic
 $vmaxcat = actcat * (kcat + 10) / 1$;Volumetric activity of Cat under substrate saturating conditions
 $actcat = 10$;U/mL ;Volumetric activity of Cat measured at 10 mM of hydrogen peroxide
 $kcat = 10$; mM ;Saturation constant for hydrogen peroxide, mM

4. Results and Discussion

In this study, nanoparticles were characterized based on their size and lifetime imaging in an open reactor. The characterization of particles' size from the Zetasizer Nano Series, was reported as follows: hydrodynamic diameter of $175\pm 1.4\text{nm}$ with an average PDI value of 0.065 for Ir(Cs)2acac, and a hydrodynamic diameter of $183\pm 1.2\text{nm}$ with an average PDI value of 0.069 for platinum porphyrin. A trustable PDI value is less and equal to 0.05 whereas 0.07 is unreliable.

Then, both particles were characterized at decreasing air nitrogen gas concentrations as air oxygen was increasing during 32 minutes. The lowest lifetime for Ir(Cs)2acac was verified to be 6 (oxygenated case or higher concentrations of oxygen) while the highest was 14 (deoxygenated case or higher concentrations of nitrogen gas) see Figure 4 (a). The lowest lifetime for platinum porphyrin was verified to be 20 (oxygenated case or higher concentrations of oxygen) while the highest was 65 (deoxygenated case or higher concentrations of nitrogen gas) see Figure 4(b). These behaviors and lifetime values matched previous studies performed at the Analytical Chemistry Institute [13]. Both particles exhibited the same behavior (quadratic) with similar coefficients of determination ($r^2=0.99$) as shown in Figure 4 (c) and (d). The main difference relies on exposure times and excitation in both cases. From these studies, Ir(Cs)2acac particles were selected as the best sensor due to these quantitative parameters previously described. In addition, this sensitive-oxygen particles were previously reported to have high solubility without aggregation and self-quenching [13]. In other words, this particular nanoparticle would reduce signal to noise ratio in measurements.

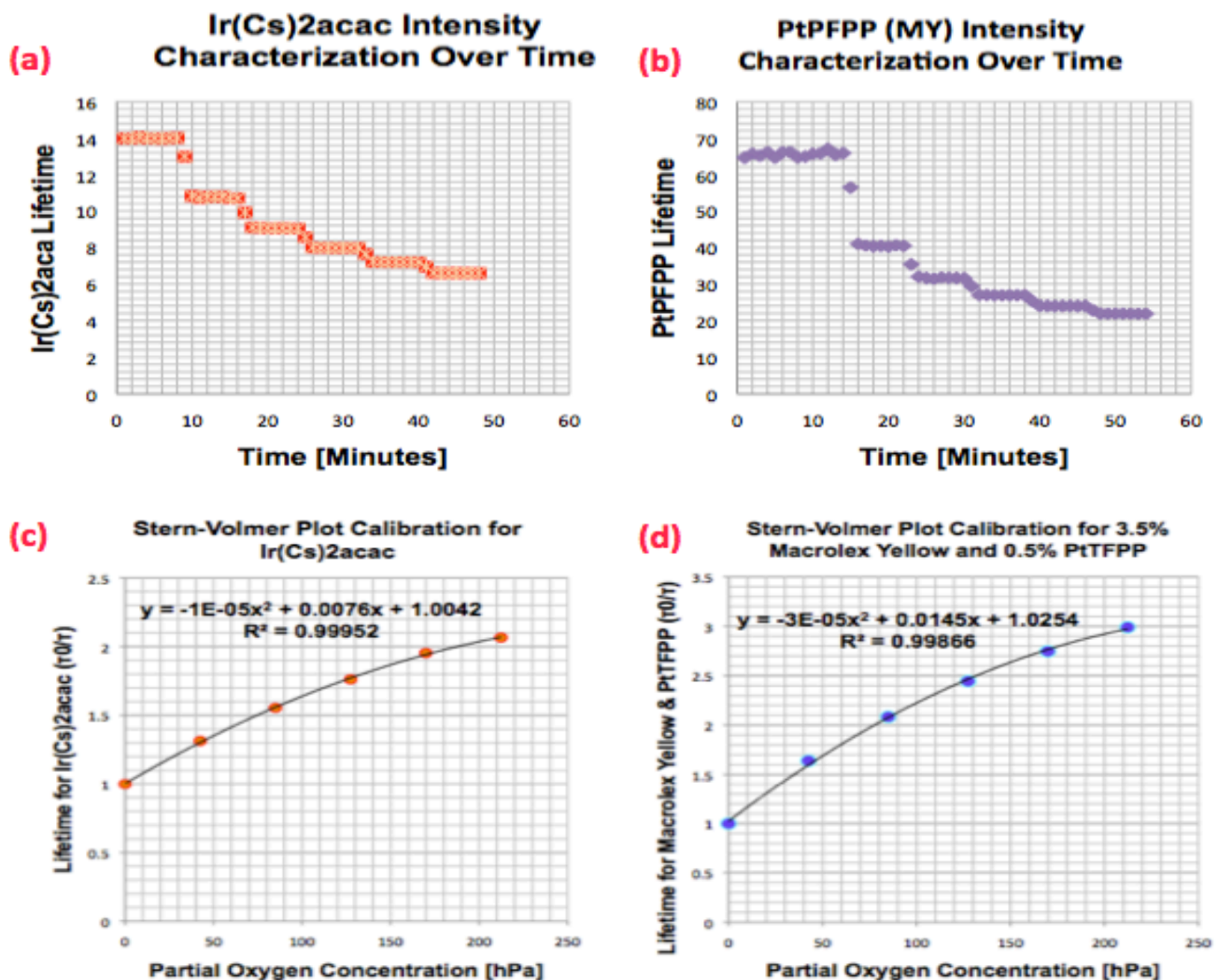


Figure 4. Particles characterization: (a) Lifetime of Ir(Cs)2acac over time in an open bioreactor (b) Lifetime of platinum porphyrin over time in an open bioreactor (c) Lifetime of Ir(Cs)2acac versus partial oxygen concentrations (d) Lifetime of platinum porphyrin versus partial oxygen concentration.

From the Berkley Maddona simulation of oxygen concentration profile and glucose conversion, it was anticipated the response of oxygen and glucose concentrations in situ. As previously described, oxygen concentration [mM] increases as hydrogen peroxide concentration [mM] increases. Contrariwise, oxygen concentration increases as glucose concentration [mM] decreases since there is an inverse relationship between glucose and hydrogen peroxide as seen in Figure 5(b). A first operation window with a flow of 1 μ L/minute, a concentration range of 0-

200mM of H_2O_2 , 0-100 units/mL of glucose oxidase, and 0-10,000 units/mL of catalase were selected from mathematical simulation (using Berkeley Madonna™). There were two simulations of importance: one simulation of oxygen concentration along the length of the microfluidic device as shown below in Figure 5 (a). In this figure, hydrogen peroxide is increasing implicitly as oxygen is depleted at the end of the continuous microreactor. Each line corresponds to a hydrogen peroxide concentration. This simulation was based on the fact that one molecule of hydrogen peroxide produces one-half molecule of oxygen.

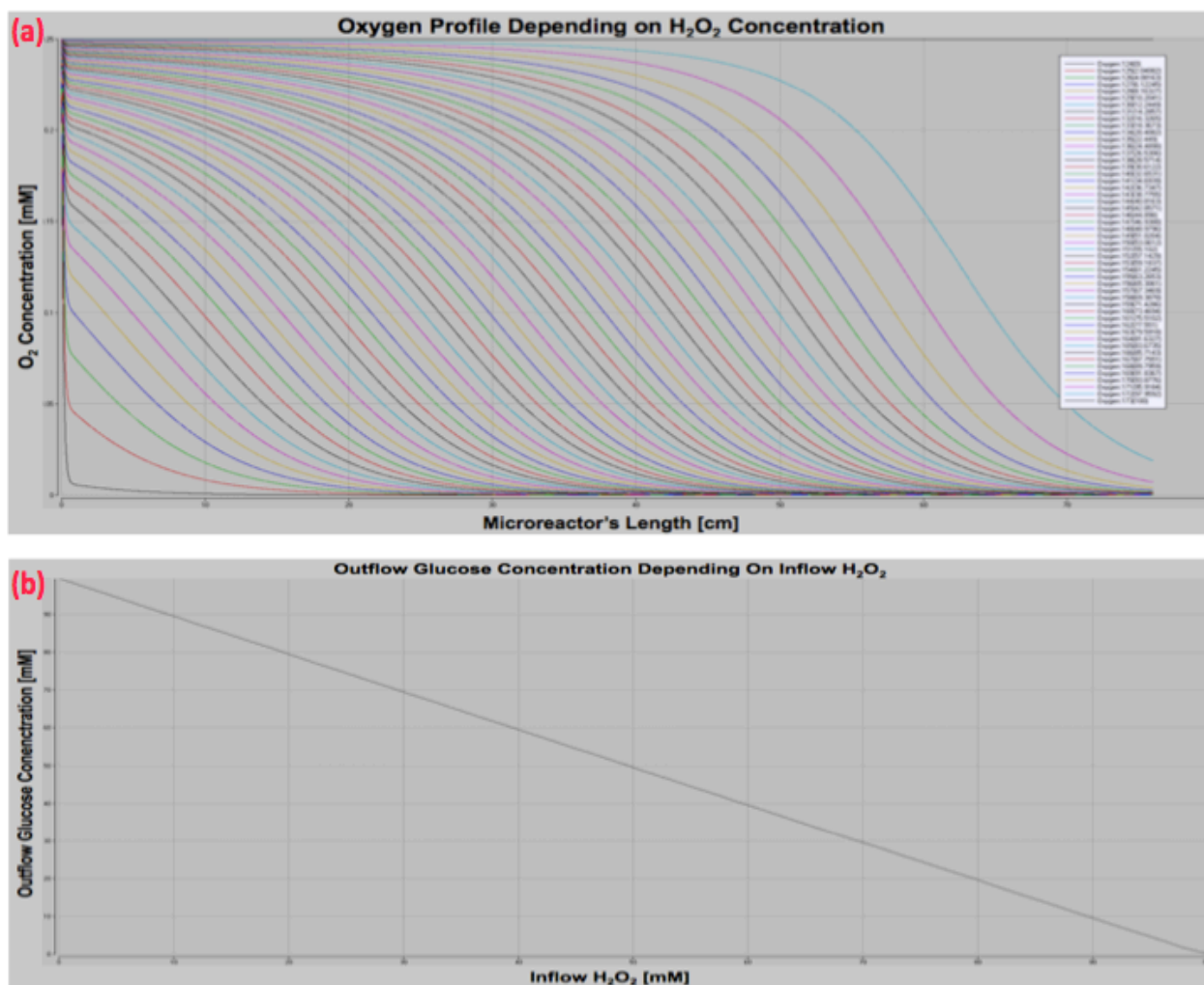


Figure 5. Berkeley Madonna Simulations: (a) Oxygen profile along continuous microreactor, (b) glucose conversion versus hydrogen peroxide.

The first operation window for measurements consisted of: 20units/mL for both GOx and catalase, 200mM glucose, and three different hydrogen peroxide concentrations (40, 80, and 200mM) with a flow rate of 1 μ L/min (steady state reached after 40 minutes of working microreactor). However, this operational window was not suitable for the needs of this study since both enzymes (GOx and catalase) were loaded on different syringes and mixing problems limited the reactions. It was evident during the deoxygenated case (only glucose loaded in one syringe along particles and GOx, plus particles loaded on the other syringe at the same ratios) that this selected window of operation was not satisfactory since the excessively long mixing time into the microchannels compromised suitability. In that case, lifetime of nanoparticles was increasing gradually up to 11. The expected results for a deoxygenated case were a lifetime of 14 for all the positions along the continuous microreactor (see Figure 4(a)). This issue was overcome by changing two key parameters of previous operational window: flow rate, activity and loading of enzymes inside syringes. Thus, the flow rate was selected to be 3 μ L/min (steady state reached after 15 minutes), and GOx and catalase activities were 60 units/mL. Both enzymes were loaded in the same syringe as well as 200mM of glucose. With this configuration the deoxygenation was quickly achieved in the microreactor when the sytemGox-glucose was used, suggesting the suitability to study the enhancement of oxygen concentration in the presence of catalase.

The analysis of glucose in the continuous microreactor was compared with the expected glucose concentrations simulated with Berkley Maddonna software. This gave researchers a better understanding of the conversion in situ. Glucose conversion was done under the presence and absence of particles. In the absence of particles, a molar coefficient extinction of 0.12 was used

to determine glucose concentration [mM]. In the presence of particles, a new calibration curve was introduced with a calculated molar coefficient extinction of 0.96. Table 1 summarized the glucose conversion results obtained after running the continuous microreactor with and without nanoparticles. It is noticeable that some measured conversions matched the expected glucose conversion when particles were not present, as opposed to 200mM of hydrogen peroxide. This mismatch of 200mM hydrogen peroxide could be explained by the saturation of the system with the generation of bubbles along the continuous microreactor. An important observation from these studies is the presence of bubbles when hydrogen peroxide concentrations are greater and equal to 100mM. This explains why glucose conversion is very low, due to higher oxygen and hydrogen peroxide concentrations.

On the other hand, when particles were present, measurements were performed at 40, 80, and 200mM hydrogen peroxide but not for the two control groups due to time limitations. For the different hydrogen peroxide concentrations, there is a remarkable difference between the expected and measured glucose conversion. Even though, for both cases were used different molar extinction coefficients (0.12 and 0.96), the expected glucose conversion should not be too divergent from the expected results. This is because particles were centrifuged for a long period of time after collecting sample solutions at a very high speed. This approach was proposed to eliminate any possibility of introducing noisy signals during absorbance measurements. In the presence of particles, for 80mM and 200mM of hydrogen peroxide there were some values that could not be calculated with MatLab since lifetime values were too small to be detected due to oxygen saturation of the system. A new method to overcome pure oxygen gas in the microfluidic device or better control and tuning of the coupled reaction rates should be addressed.

Experimental Groups	Inlet 1 Flow [$1\mu\text{L}/\text{min}$]	Inlet 2 Flow [$1\mu\text{L}/\text{min}$]	Expected Glucose Concentration	Measured Glucose Concentration No Particles; 0.12 Molar extinction Coefficient	Measured Glucose Concentration With Particles 0.96 Molar extinction Coefficient
Control 1	200mM Glucose + Particles	50mM K_3PO_4 + Particles	100 mM	100 mM	-----
Control 2	200mM Glucose + Particles	20 Units/mL Gox + Particles	99.75 mM	88.5 mM	-----
40mM H_2O_2	200mM Glucose + 40mM H_2O_2 + Particles	20 U/mL Gox + 20 U/mL Catalase + Particles	80mM	45mM	16.33mM *(60units/mL of enzymes)
80 mM H_2O_2	200mM Glucose + 80mM H_2O_2 + Particles	20 U/mL Gox + 20 U/mL Catalase + Particles	60 Mm	76.48 Mm	9.27mM *(60units/mL of enzymes)
200 mM H_2O_2	200mM Glucose + 200mM H_2O_2 + Particles	20 U/mL Gox + 20 U/mL Catalase + Particles	0.0405mM	49.7mM	8.62mM *(60units/mL of enzymes)

Table 1. Summarizes glucose conversion inside the continuous microreactor under the presence and absence of particles. When particles were not present, most of the experimental data matched the expected results as opposed to the cases when particles were present.

For real time in situ oxygen measurements, the preliminary results for lifetime are displayed in Figure 6. In this figure, it is visible that per each position along the continuous microreactor, there is a representative picture of 3 microchannels (light blue traces). This color code varies from 0 to 40, and the range for Ir(Cs)2acac nanoparticles remained in the blue region. However, for 200mM of hydrogen peroxide is hard to see these channels since lifetime could not be detected with the analytical technique and therefore oxygen concentration could be determined. Only the final position in the microchannel for 200mM hydrogen peroxide showed some microchannels. This is mainly due to the higher bubble production inside the device. In addition, the scripts of MatLab were coded to only detect the highest and lowest intensities, normalize them, and provide the mean and standard deviation values.

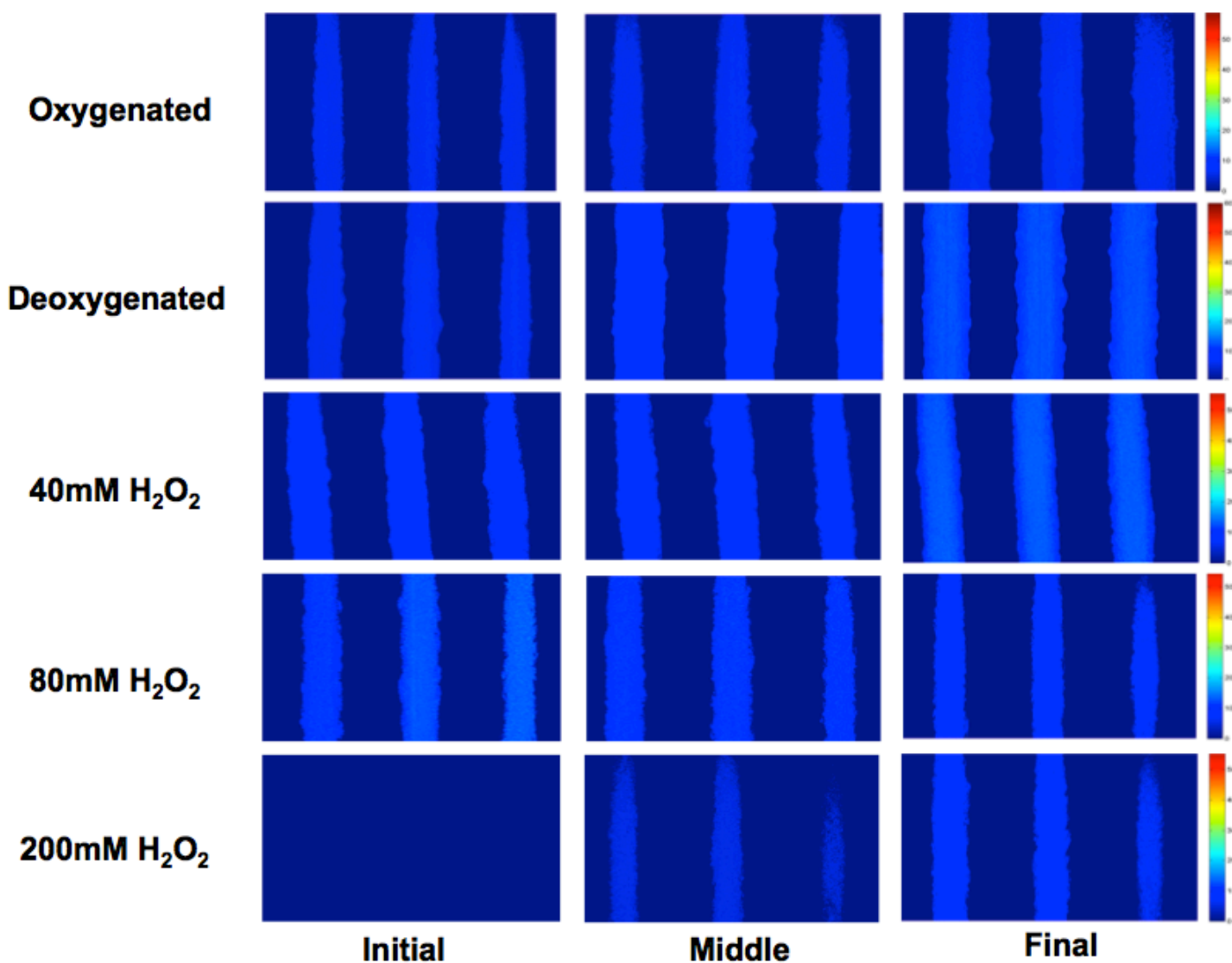


Figure 6. Representation of oxygen lifetime imaging for each set condition along three positions of the continuous microreactor. These images were analyzed and generated through MatLab.

Under the same operational window were performed the oxygenated and the first deoxygenated case: 20units/mL for GOx and catalase, and a flow rate of 1 μ L/min as shown in Table 2. For the oxygenated condition, values for oxygen were reported to be within the range of 314-327 μ mol/L. These values were completely saturated as expected. For the deoxygenated condition, there was a trend of lifetime images to increase along the continuous microreactor. This finding was not expected since the habitual lifetime for Ir(Cs)2acac was about 14 for deoxygenated conditions.

This indicated that somehow the operational window should be changed. Thus, the flow rate and enzyme activities were increased three times, and GOx and glucose were pre-mixed in the same syringe. This experiment was repeated under the new conditions. For the new deoxygenated case, lifetime values were close to 14, which indicated low oxygen concentrations as expected (16-32 $\mu\text{mol/L}$). For 40mM of hydrogen peroxide reported higher oxygen values at the inlet (123 $\mu\text{mol/L}$) than at the outlet (23 $\mu\text{mol/L}$) displaying a progressive oxygen consumption along the microreactor. Likewise, for 80mM hydrogen peroxide was reported similar findings (75-134 $\mu\text{mol/L}$). These findings were slightly contradicting, since it was expected higher oxygen concentrations at the end of the microreactor from the Berkley Madonna Simulation along the length of the microfluidic device. The velocity of oxygen consumption by Gox might be higher than expected or the catalase catalyzed oxygen generation lower than required. For 200mM, there were reported a variety of results due to a system oversaturated with oxygen. The signal to noise ratio was too high due to bubble generation, and lifetime of initial position could not be detected with MatLab. For the lifetime of middle position, the concentrations of oxygen were out of range of the calibration curve generated with the open bioreactor. For the final position, some oxygen concentration was reported but it is not as expected.

Case	Microreactor position	Lifetime	T/To	O ₂ [hPa]	O ₂ [μmol/L]
	Intial	6.3	2.22	230	314
Oxygenated (20units/mL)	Middle	6.16	2.27	236	320
	Final	6.03	2.32	242	327
	Intial	6.31	2.23	231	327.7
Deoxygenated (20units/mL)	Middle	8	2.27	120	163.8
	Final	11.36	2.32	30	40.9
	Intial	12.6	1.11	12.5	17.07
Deoxygenated (60 Units/mL)	Middle	12.75	1.1	12	16.38
	Final	11.81	1.19	24	32.77
	Intial	8.78	1.6	90	122.87
40mM H₂O₂ (60 Units/mL)	Middle	11.68	1.2	25	34.13
	Final	12.29	1.14	17	23.21
	Intial	8.6	1.63	98	133.79
80mM H₂O₂ (60 Units/mL)	Middle	10.04	1.4	55	75.09
	Final	9.56	1.46	65	88.74
	Intial	N/A	N/A	*Saturated	*Saturated
200mM H₂O₂ (60 Units/mL)	Middle	4.86	2.88	Out Range	Out Range
	Final	9.51	1.47	66	90.1

Table 2. Summarizes all lifetime values with their respective oxygen concentration per position.

5. Conclusions and outlook

Ir(Cs)₂acac particles with a simple preparation procedure were selected because of their high brightness under small amount of excitation (470nm) which allowed reliable signals even in the complex medium made of substrates, enzymes, and by-products of glucose oxidation. These oxygen sensitive particles were compatible with the reaction conditions since oxygen was generated in situ without any interference with the particles medium. These particles were promising for monitoring lifetime imaging microscopy based on the preliminary results of the study.

The preliminary conditions obtain from Berkley Madonna simulation were found to be useful to understand oxygen generation in situ. The key point of success consist of balancing enzymes activity as well as tuning them with the best suitable flow rate and loading strategy of substrate (glucose), enzymes (GOx, and catalase), by-product (hydrogen peroxide), and particles (Ir(Cs)₂acac) in a continuous microreactor. Another important strategy in this study was changing the loading of enzymes inside syringes (all together: glucose, GOx, catalase, and particles). At the other syringe, during the loading time hydrogen peroxide was not affected by catalase or GOx. In this study, in situ oxygen feeding for optimal oxidation was achieved through new operational window conditions established.

Even though oxygen generation in situ was achieved successfully, there is an emergent need to introduce a new method to prevent Ir(Cs)₂acac particles to interfere with the glucose conversion results. Centrifugation for long time and at higher rates was introduced to prevent the previous issue but still a better calibration curve to measure NADH absorbance under the presence of

particles is required. In addition, oxygen conversion was affected by particles presence as shown in Table 2.

Future approaches to continue understanding oxygen generation in microfluidic devices includes, the ratiometric approach under the established operational window, and thus correlate intensity values with oxygen concentration at different positions along the chip. This would be possible through fluorescence microscopy and a color camera as described before [9]. The end goal consists of immobilization of enzymes as well as local glucose concentration measurements. It would be interesting to extend this technology of local oxygen concentration resolution in addition to the strategy of in situ oxygen concentration generation with immobilization of enzymes. This is because immobilized enzymes in continuous microreactors represent an important use for biotechnology applications. There is a emergent interest to monitor oxidations catalyzed by immobilized oxidases using local measurements, particularly since the oxidation catalyzed by immobilized enzymes might offer a major oxygen limitation

6. Acknowledgements

First of all, I would like to thank Prof. Bernd Nidetzky for the opportunity to allow me to work under his mentorship during this summer 2013 at the Institute of Biotechnology and Biochemical Engineering – Graz University of Technology (TU Graz).

Secondly, I want to express my deepest gratitude to Dr. Juan M. Bolivar for his guidance, help and time offered to me through my whole internship at TU Graz. Thanks to his extensive training and mentorship, I was able to achieve important skills in enzymatic reactions, microfluidic devices, and essential measurements in biotechnology related to oxygen imaging. The success of the preliminary results for this started up project was due in large extend to his experience and foreknowledge.

I also would like to thank Prof. Torsten Mayr from the Institute of Analytical and Food Chemistry – Graz University of Technology, and two of his graduate students (Birgit Ungerböck and Josef Ehgartner) for their guidance and support as well as for allowing me to use their optical equipment to perform oxygen-imaging measurements.

Last but not least, I would like to thank the generosity of the Austrian Marshall Plan Foundation for their financial support, which allowed me to conduct research abroad. This experience enabled me to grow as a young researcher as well as a person.

7. References

1. Sud, D., et al., *Optical imaging in microfluidic bioreactors enables oxygen monitoring for continuous cell culture*. J Biomed Opt, 2006. **11**(5): p. 050504.
2. Gao, F.G., et al., *Optical sensor based on fluorescent quenching and pulsed blue LED excitation for long-term monitoring of dissolved oxygen in NASA space bioreactors*. J Biomed Opt, 2005. **10**(5): p. 054005.
3. Christensen, D.A. and J.N. Herron, *Optical system design for biosensors based on CCD detection*. Methods Mol Biol, 2009. **503**: p. 239-58.
4. Mehta, G., et al., *Quantitative measurement and control of oxygen levels in microfluidic poly(dimethylsiloxane) bioreactors during cell culture*. Biomed Microdevices, 2007. **9**(2): p. 123-34.
5. Garcia-Ochoa, F., E.G. Castro, and V.E. Santos, *Oxygen transfer and uptake rates during xanthan gum production*. Enzyme Microb Technol, 2000. **27**(9): p. 680-690.
6. Miyazaki, M., et al., *Enzymatic processing in microfluidic reactors*. Biotechnol Genet Eng Rev, 2008. **25**: p. 405-28.
7. Bolivar, J.M., et al., *Shine a light on immobilized enzymes: real-time sensing in solid supported biocatalysts*. Trends Biotechnol, 2013. **31**(3): p. 194-203.
8. Bolivar, J.M., et al., *Quantitating intraparticle O₂ gradients in solid supported enzyme immobilizates: experimental determination of their role in limiting the catalytic effectiveness of immobilized glucose oxidase*. Biotechnol Bioeng, 2013. **110**(8): p. 2086-95.
9. Ungerbock, B., et al., *Microfluidic oxygen imaging using integrated optical sensor layers and a color camera*. Lab Chip, 2013. **13**(8): p. 1593-601.
10. Bolivar, J.M., Nidetzky, B., *Smart enzyme immobilization in microstructured reactors*, in *Chimica Oggi/Chemistry Today*. 2013. p. 50-54.
11. Bolivar, J.M., J. Wiesbauer, and B. Nidetzky, *Biotransformations in microstructured reactors: more than flowing with the stream?* Trends Biotechnol, 2011. **29**(7): p. 333-42.
12. Ungerböck, B., et al., *Online oxygen measurements inside a microreactor with modeling of transport phenomena*. Microfluidics and Nanofluidics, 2012. **14**(3-4): p. 565-574.
13. Borisov, S.M. and I. Klimant, *Luminescent nanobeads for optical sensing and imaging of dissolved oxygen*. Microchimica Acta, 2008. **164**(1-2): p. 7-15.
14. Borisov, S.M. and I. Klimant, *Ultrabright oxygen optodes based on cyclometalated iridium(III) coumarin complexes*. Anal Chem, 2007. **79**(19): p. 7501-9.
15. Borisov, S.M., G. Zenkl, and I. Klimant, *Phosphorescent platinum(II) and palladium(II) complexes with azatetrabenzoporphyrins-new red laser diode-compatible indicators for optical oxygen sensing*. ACS Appl Mater Interfaces, 2010. **2**(2): p. 366-74.
16. Pfeiffer, M., *Controlled Oriented Immobilization of Catalase to Overcome Oxygen Diffusional Limitations*, in *Institute of Biotechnology and Biochemical Engineering 2012*, Graz University of Technology: Graz, Austria. p. 38.
17. Consolati, T., *Time and Space Resolved Oxygen Imaging of Oxidases Immobilized Onto Porous Carriers*, in *Institute of Biotechnology and Biochemical Engineering*. 2012, Graz University of Technology Graz, Austria. p. 32.
18. Moser, C., T. Mayr, and I. Klimant, *Microsphere sedimentation arrays for multiplexed bioanalytics*. Analytica Chimica Acta, 2006. **558**(1-2): p. 102-109.

19. Moser, C., *Multiplexed Bioanalysis: Sedimentation Arrays Based on Luminescently Encoded Magnetic Microspheres*, in *Institute of Analytical Chemistry and Radiochemistry*. 2011, Graz University of Technology: Graz, Austria. p. 152.
20. Ltd., M.I. *Zetasizer Nano Series User Manual*. 2004; Available from: <http://www.nbtc.cornell.edu/facilities/downloads/Zetasizer%20Manual.pdf>.
21. Petzelbauer I., N.B., Haltrich D., Kulbe K. D., *Development of an ultra-high-temperature process for the enzymatic hydrolysis of lactose. I. The properties of two thermostable β -glycosidases*. *Biotechnology and Bioengineering*, 1999. **64**: p. 322-332.
22. Liebsch G., K.I., Frank B., Holst G., Wolfbeis O.S., *Luminescence Lifetime Imaging of Oxygen, pH, and Carbon Dioxide Distribution Using Optical Sensors*. *Applied Spectroscopy*, 2000. **54**(4): p. 548-559.